Virologica Sinica (2021) 36:1197–1209
https://doi.org/10.1007/s12250-021-00407-6

www.virosin.org
www.springer.com/12250

RESEARCH ARTICLE

Modulation of Antiviral Immunity and Therapeutic Efficacy by 25-Hydroxycholesterol in Chronically SIV-Infected, ART-Treated Rhesus Macaques

Chunxiu Wu[1,4] · Jin Zhao[2,3] · Ruiting Li[2,3] · Fengling Feng[2,3] · Yizi He[1,4] · Yanjun Li[2,3] · Runhan Huang[2] · Guangye Li[8] · Heng Yang[5,6] · Genhong Cheng[5,6,7] · Ling Chen[1,4] · Feng Ma[5,6] · Pingchao Li[1] · Caijun Sun[2,3]

Received: 29 January 2021 / Accepted: 19 April 2021 / Published online: 31 May 2021

Abstract

Cholesterol-25-hydroxylase (CH25H) and its enzymatic product 25-hydroxycholesterol (25HC) exert broadly antiviral activity including inhibiting HIV-1 infection. However, their antiviral immunity and therapeutic efficacy in a nonhuman primate model are unknown. Here, we report that the regimen of 25HC combined with antiretroviral therapy (ART), provides profound immunological modulation towards inhibiting viral replication in chronically SIV_{mac239}-infected rhesus macaques (RMs). Compared to the ART alone, this regimen more effectively controlled SIV replication, enhanced SIV-specific cellular immune responses, restored the ratio of CD4/CD8 cells, reversed the hyperactivation state of $CD4^+$ T cells, and inhibited the secretion of proinflammatory cytokines by $CD4^+$ and $CD8^+$ T lymphocytes in chronically SIV-infected RMs. Furthermore, the *in vivo* safety and the preliminary pharmacokinetics of the 25HC compound were assessed in this RM model. Taken together, these assessments help explain the profound relationship between cholesterol metabolism, immune modulation, and antiviral activities by 25HC. These results provide insight for developing novel therapeutic drug candidates against HIV-1 infection and other related diseases.

Keywords 25-hydroxycholesterol (25HC) · HIV · SIV · Antiretroviral therapy (ART) · Macaque

Introduction

The human immunodeficiency virus (HIV)/Acquired Immune Deficiency Syndrome (AIDS) epidemic, one of the most severe challenges in the field of public health, is still rampant worldwide. Approximately 38 million

Supplementary Information The online version contains supplementary material available at https://doi.org/10.1007/s12250-021-00407-6.

✉ Caijun Sun
suncaijun@mail.sysu.edu.cn

✉ Pingchao Li
li_pingchao@gibh.ac.cn

✉ Feng Ma
maf@ism.pumc.edu.cn

[1] State Key Laboratory of Respiratory Disease, Guangzhou Institutes of Biomedicine and Health (GIBH), Chinese Academy of Sciences, Guangzhou 510530, China

[2] School of Public Health (Shenzhen), Sun Yat-Sen University, Guangdong 518107, China

[3] Key Laboratory of Tropical Disease Control, Sun Yat-Sen University, Ministry of Education, Guangzhou 514400, China

[4] University of Chinese Academy of Sciences, Beijing 100049, China

[5] Center for Systems Medicine, Institute of Basic Medical Sciences, Chinese Academy of Medical Sciences and Peking Union Medical College, Beijing 100005, China

[6] Suzhou Institute of Systems Medicine, Suzhou 215123, China

[7] Department of Microbiology, Immunology and Molecular Genetics, University of California, Los Angeles 90095, USA

[8] Guangdong Landau Biotechnology Co. Ltd, Guangzhou 510700, China

individuals live with HIV/AIDS nowadays (UNAIDS). Antiretroviral therapy (ART) can effectively inhibit HIV replication, and it has turned AIDS from a fast-fatal incurable disease to a manageable chronic disease. However, ART cannot fully cure HIV-related clinical symptoms, such as persistent inflammation, extensive immune activation, and abnormal lipid metabolism (Churchill *et al.* 2016; Koethe *et al.* 2020; Premeaux *et al.* 2020). Approximately 40% of HIV-infected patients suffer from dyslipidemia (Grand *et al.* 2020), resulting in an increased incidence of cardiovascular disease with a 1.5 to 1.7 times higher risk than that of the general population (Freiberg *et al.* 2013). Considering that an estimated 25.4 million AIDS patients are currently receiving life-long ART, it is becoming increasingly important to regulate lipid metabolism disorders in long-term ART-treated HIV patients. The American Infectious Diseases Association has added relevant items to *the Guide for Primary Care of HIV-Infected Persons* (Aberg *et al.* 2014). As a result, researchers are exploring novel antiviral drugs that can simultaneously reshape immune function, repress viral replication, and restore normal physiological metabolic balance, to achieve the coordinated control and the eventual elimination of HIV infection.

Cholesterol-25-hydroxylase (CH25H), also known as cholesterol-25-monooxygenase, belongs to the redox enzyme family, and it can catalyze cholesterol to produce 25-hydroxycholesterol (25HC), an oxidative product of cholesterol metabolism that is closely related to the regulation of lipid metabolism (Lund *et al.* 1998). CH25H and 25HC have been regarded as important regulators that maintain cholesterol homeostasis by inhibiting sterol regulator-binding protein (SREBP) and liver X receptor (LXR) (Lehmann *et al.* 1997; Radhakrishnan *et al.* 2004). Recently, CH25H and 25HC have also been shown to play critical roles in the regulation of inflammation, innate immunity, and subsequent adaptive immune responses through interferon signaling (Glass and Saijo 2010; Ludigs *et al.* 2012; Spann and Glass 2013; Zhao *et al.* 2020). Furthermore, CH25H and 25HC have been found to inhibit a variety of viruses, including Zika virus (ZIKV) (Li *et al.* 2017), HIV-1, human herpesvirus 1 (HSV-1), hepatitis C virus (HCV), Ebola virus (EBoV) (Liu *et al.* 2013; Doms *et al.* 2018), Lassa virus (Shrivastava-Ranjan *et al.* 2016), rabies virus (Yuan *et al.* 2019), and SARS-CoV-2 (Zu *et al.* 2020). Our recent study also indicated that 25HC treatment significantly suppressed simian immunodeficiency virus (SIV) infection by modulating both innate and adaptive immune responses in a dose-dependent manner *in vitro*, and enhanced SIV-specific IFN-γ-producing cellular responses but selectively suppressed proinflammatory $CD4^+$ T lymphocytes in immunized mice with the SIV vaccine (Wu *et al.* 2018). Given the multifaceted functions of 25HC, this compound warrants exploration as a potential therapeutic drug in preclinical and clinical studies. Further, its antiviral immunity and therapeutic efficacy in a non-human primate model are unknown.

In the present study, we investigated how 25HC affects viral replication, lipid metabolism, and immune modulation in a chronically SIV-infected, long-term ART-treated RM model. We also explored the *in vivo* safety of 25HC in this nonhuman primate model. This study helps us understand the relationship between cholesterol metabolism, immune modulation, and antiviral activities by 25HC, and provides insight for developing novel therapeutic drug candidates against HIV infection and other related diseases.

Material and Methods

Drugs, SIV Peptide Pools, and Virus

25HC was kindly provided by Prof. Genhong Cheng and Feng Ma, and dissolved in ethanol, and stored at –20 °C.

Reverse Transcriptase Inhibitors: (R)-9-(2-phosphonylmethoxypropyl) adenine (PMPA, also called tenofovir) and beta- 2, 3-dideoxy-3-thia-5- uorocytidine (FTC, also called emtricitabine) were provided by Shanghai Desano Pharmaceutical Co., Ltd. These drugs were provided in powder formation of active pharmaceutical ingredient, and dissolved in 0.9% saline solution to a final concentration as below.

Peptide pools, which covered the entire SIV_{mac239} sequences of Gag, Pol, Env, Nef, Vif, Vpx, Vpr, Rev, and Tat proteins, were obtained through the AIDS Research and Reference Reagent Program, National Institutes of Health (NIH), USA. Peptide pools consisted of 15 amino acids shifted by 11 overlapping amino acids residues, and dissolved in dimethyl sulfoxide to a final concentration of 0.4 mg per peptide mL^{-1} before use. Concanavalin A (ConA, Sigma), ionomycin (Ion, Sigma) and phorbol myristate acetate (PMA, Enzo Biochem, Inc.) were prepared and stored according to the manufacturer's instructions.

The original SIV_{mac239} stock was obtained through the AIDS Research and Reference Reagent Program, National Institutes of Health (NIH), USA. The challenge stock was propagated and purified in peripheral blood mononuclear cells (PBMCs) of rhesus macaques (RMs) and tittered in 174×CEM cells in our lab.

Animals and Ethical Statement

Chinese RMs were housed in the Experimental Animal Center of Guangzhou Institutes of Biomedicine and Health (GIBH, Guangzhou, China). All procedures were

performed by trained personnel under the supervision of veterinarians. Eleven RMs were recruited in this study and assigned to one of two treatment groups: 25HC combined with ART or ART-only. Briefly, all 11 RMs were intravenously inoculated with 5000 50% tissue culture infectious dose (TCID50) SIV at 0 days post infection (dpi) and received antiretroviral therapy (FTC/20 mg/kg/once daily + PMPA/30 mg/kg/once daily) from 69 to 132 dpi. During this period, 6 RMs in the 25HC+ART group received daily intravenous infusion of 25HC (1.5 mg/kg) from 119 dpi ~ 125 dpi, and the RMs in the ART-only group received intravenous drip vehicle (ethanol). To further study the therapeutic effect of 25HC alone, we also performed an additional week with 25HC treatment alone in these RMs of the 25HC + ART group, and the RMs of the ART-only group were given ethanol. Samples were collected to monitor the virological and immunological parameters following the experimental schedule, as shown in Fig. 1.

Immunological Assays

PBMCs from SIV-infected RMs were isolated by standard Ficoll-Hypaque density gradient centrifugation, and then used for IFN-γ ELISPOT assay and intracellular cytokine staining (ICS) assay as we described previously (Sun *et al.* 2010; Pan *et al.* 2018). For IFN-γ ELISPOT assay, freshly isolated PBMCs were added at 4×10^5 cells/well in anti-RM IFN-γ monoclonal antibody (BD Pharmingen) pre-coated 96-well plates containing Immobilon-P membrane (Millipore, USA). SIV peptide pools were added into cells for 20–24 h for stimulation, and then a polyclonal anti-RM IFN-γ biotinylated detector antibody (BD Pharmingen) was added. The next day, the plates were washed and color was

A

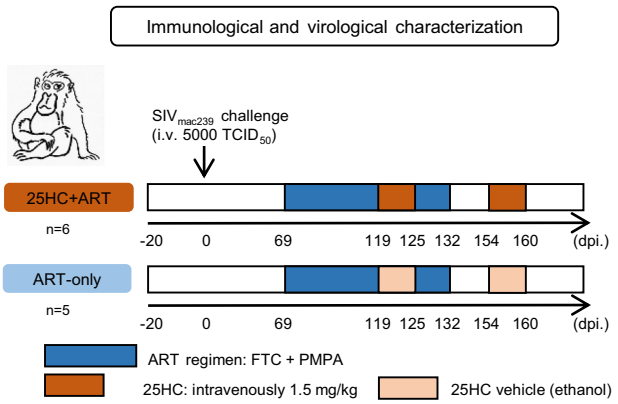

B

Group	Animal ID	Sex	Weight(Kg)	Age(year)
ART-only	80126	F	7.85	10
	120290	F	6.98	6
	031669R	M	9.21	15
	80159	M	10.32	10
	41646	F	5.87	14
25HC+ART	R070115	M	13.75	11
	120294	F	5.93	6
	120316	F	5.22	6
	80017	M	11.25	10
	04086	F	4.23	14
	124352	F	6.16	6

C

Time(dpi)	-20	0	42	62	69	76	83	95	119	126	138	152	154	161
SIV challenge														
ART treatment														
25HC or vehicle														
Viral load test														
PBMC collection														
Blood biochemical														
Complete blood count														
25HC metabolism														

Fig. 1 The experimental schedule and specimen collection in this study. **A** Eleven rhesus macaques were randomly assigned into two groups: the 25HC combined with ART group and the ART-only group. All rhesus macaques were intravenously injected with 5000 TCID50 (50% tissue culture infectious dose) SIV at day 0 (black arrow), and daily ART administration (blue shaded area) was started at 69 dpi (day post infection). The 6 macaques in the 25HC+ART group were intravenously dripped with 25HC (red shaded area) from 119 to 125 dpi, and the 5 rhesus macaques in the ART-only group were injected with vehicle (ethanol) at the same time. ART was interrupted at 132 dpi. At 154 dpi, the 25HC+ART group was infused with 25HC alone, and the ART-only group was injected with vehicle (ethanol). **B** Information on rhesus macaques enrolled in this study. **C** The schedule of specimen collection, including the time-points for SIV challenge, ART, 25HC treatment, plasma viral load detection, PBMC collection, blood biochemistry, complete blood count, and 25HC pharmacokinetic analysis. Dpi = days post infection.

developed by incubating in NBT/BCIP (Pierce, Rockford, IL) for 10 min. Spots were counted under an ELISPOT reader (Bioreader 4000, BIOSYS, Germany), and data were reported as the number of spot-forming cells (SFCs) per million PBMCs. Concanavalin A stimulation was used as a positive control in the ELISPOT assay.

For ICS assay, 10^6 cells were stimulated with SIV peptides for 2 h, and then brefeldin A (BD Biosciences) was added for an additional 16 h. The cells were then washed and stained for 30 min with anti-CD3–Pacific Blue, anti-CD4–PE-CF594, anti-CD8–allophycocyanin (APC)–Cy7, anti-CD28–fluorescein isothiocyanate (FITC), and anti-CD95–phycoerythrin (PE)–Cy5. Next, the cells were suspended in 250 μL of Cytofix/Cytoperm solution (BD Pharmingen) for 20 min, washed with Perm/Wash solution (BD Pharmingen), and intracellularly stained with anti-IFN-γ–PE, anti-TNF-α–PE–Cy7 and anti-IL-2-APC (BD Pharmingen) for 30 min. Samples were analyzed with BD LSRFortessa™ (BD Biosciences) instrument and FlowJo software (Tree Star, Inc). PMA/I (phorbol myristate acetate + ionomycin) stimulation was used as a positive control in the ICS assay. The antibodies used in this study for analytical flow cytometry are listed in Supplementary Table S1.

For cell activation detection, PBMCs were detected with the following monoclonal antibodies: anti-CD3-PerCP, anti-CD4-FITC, anti-CD4-APC, anti-CD38-FITC, anti-CD25-APC, anti-CD69-PE, anti-CD95-PE-Cy5, anti-Ki67-PE, and anti-CCR5-PE. Samples were analyzed with an Accuri C6 flow cytometer (BD Biosciences) and FlowJo software (version 10; Tree Star, Inc.).

Viral Load Determination by Real-Time PCR

The SIV RNA copies in plasma were quantitated by real-time PCR as described previously (Wong *et al.* 1997; Kimata *et al.* 2016). Briefly, viral RNA was extracted from plasma using the QIAamp Viral RNA Minikit (Qiagen), and then quantitated using the QuantiTect SYBR Green RT-PCR Kit (Qiagen) with LightCycler480 II Real-time PCR system (Roche). Primers were designed to match the SIV_{mac239} *gag* sequence. The copy number of viral RNA was calculated based on the standard curve of an *in vitro*-transcribed fragment of the SIV_{mac239} *gag* gene. The limitation for this assay was 100 copies mL^{-1} plasma. Sequences of all primers used in this study were listed in Supplementary Table S2.

The Complete Blood Count, Blood Biochemical Test, and the Preliminary Pharmacokinetics of 25HC in Rhesus Macaques

Peripheral blood and plasma samples were collected following standard protocols, and the complete blood count and biochemical tests were performed with Sysmex automatic modular animal blood and body fluid analyzer XN-1000 V and Hitachi Automatic Aralyzer 3100 by Guangdong Laboratory Animals Monitoring Institute.

To study the preliminary pharmacokinetics of 25-hydroxycholesterol, lipids were extracted from plasma samples using an improved Bligh/Dyer extraction method (two extractions). The lipids were dried in a vacuum rotary thickener and then remelted in an ethanol and isotope mixture containing 1% (W/V) butylated hydroxytoluene (BHT). The lipids were incubated at 37 °C for 1 h, deionized water and ethanol were added, and the samples were incubated for another 15 min. Subsequently, the upper organic phase was obtained by centrifugation, and pyridine acid derivatization was carried out. After derivatization, a liquid-mass spectrometer (Exion UPLC-QTRAP 6500 PLUS, Sciex) was used for analysis, and electrospray ionization (ESI) mode was used for quantitative analysis. The isotopic internal standard is d_6-25-hydroxycholesterol.

Data Analysis

Flow cytometry software analysis was performed using FlowJo 10 (Tree Star Inc.). Graphical representations were generated with GraphPad Prism 8 (GraphPad Software Inc., La Jolla, CA) and IBM SPSS Statistics 25.0. Two-tailed P values were calculated, and differences were considered as statistically significant when $P < 0.05$.

Results

Animal Model and Experimental Design

To explore the effect of 25HC on the SIV-infected RM model, we designed the following experiments (Fig. 1A). Eleven RMs were recruited and assigned into two groups based on body weight (4–13 kg), sex, age (6–15 years old), and initial immune status (Fig. 1B): 25HC combined with ART administration group (25HC + ART), and ART-alone administration group (ART-only). All 11 RMs were intravenously inoculated with 5000 50% tissue culture infectious dose (TCID50) SIV at 0 days post infection (dpi), and received antiretroviral therapy (FTC/20 mg/kg/once daily + PMPA/30 mg/kg/once daily) from 69 to 132 dpi. During this period, 6 RMs in the 25HC + ART group

received daily intravenous infusion of 25HC (1.5 mg/kg) from 119 dpi ∼ 125 dpi, and the RMs in the ART-only group received intravenous infusion of vehicle (ethanol). To study the therapeutic effect of 25HC alone, we performed an additional week of 25HC administration. The experimental operation and specimen collection of RMs in this study are shown in Fig. 1C.

25HC Combined with ART Might be Helpful in Controlling Viremia in SIV-Infected RMs

Enzymatic product 25HC has been reported to inhibit a variety of viruses (Zhao *et al.* 2020). Thus, we sought to evaluate its effect on SIV replication in the RM model. At 56 dpi, the median level of plasma viral load in all RMs was 4.3 lg (copies/mL) (range 3.9–5.4 lg). After initializing ART at 69 dpi, the plasma viral load in all RMs rapidly decreased until it was undetectable (Fig. 2A, 2B). Interestingly, at 126 dpi (the 58th day of ART), the plasma viral load of two RMs in the ART-only group rebounded to 4.7 and 3.9 lg (copies/mL) respectively, accounting for 40% of animals in this group. However, only one RM in the 25HC+ART group rebounded to 4.0 lg (copies/mL), accounting for 16.67% of animals in this group (Fig. 2C). There was no statistically significant difference in the viral rebound ratio between the two groups, possibly due to the small number in this study.

The plasma viral load of all RMs was monitored before ART and after ART termination. We noticed that the fold changes of peak plasma viral load relative to baseline were lower in the 25HC+ART group (Fig. 2D). In addition, the average set-point of plasma viral load in the 25HC + ART group was 4.5 lg (copies/mL) before treatment, and rebounded to 3.9 lg (copies/mL) after drug withdrawal, which was significantly lower than the viral load before treatment. However, there was no significant change between plasma viral load before ART and after ART termination in the ART-only group (Fig. 2E). We next wondered whether 25HC treatment alone could also play a role in controlling plasma viral load (Fig. 1A), but we found no significant change in plasma viral load with or without 25HC treatment alone (Fig. 2A and 2B). Overall,

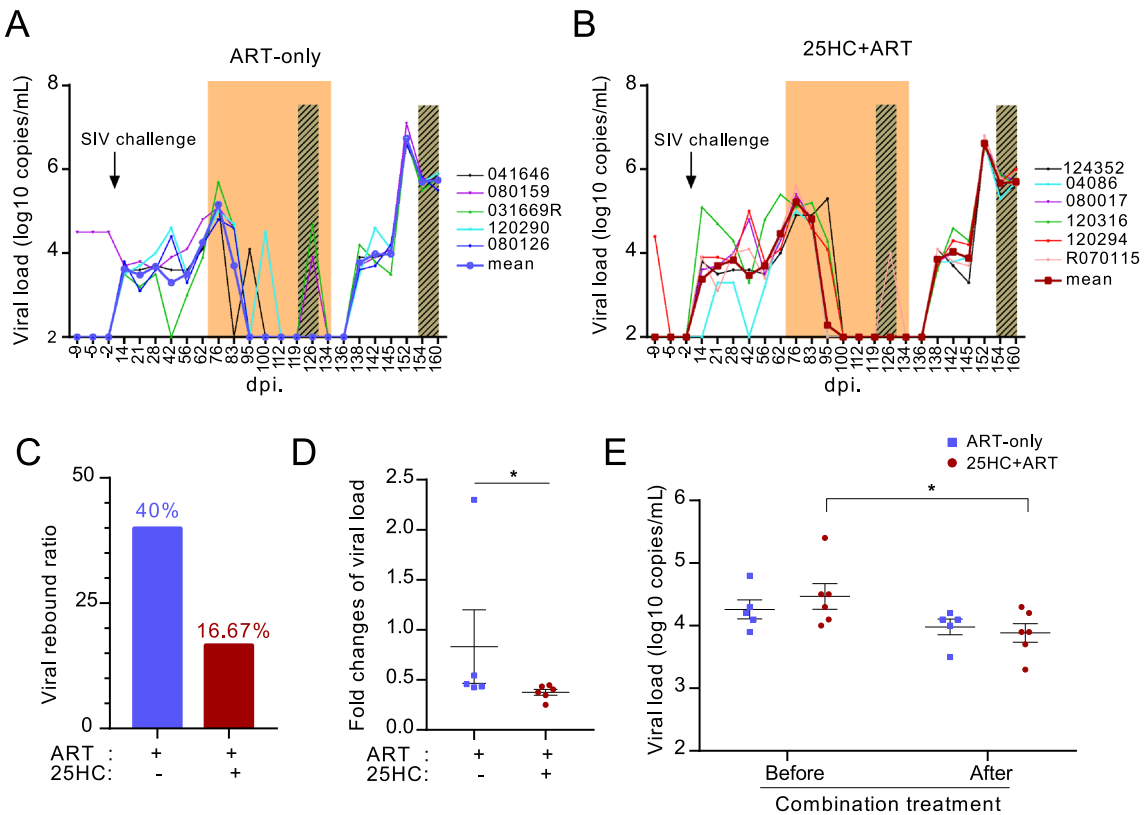

Fig. 2 25HC combined with ART improved the control of viral replication in SIV-infected RMs. **A**, **B** Plasma viral load in the ART-only group (n = 5) and 25HC + ART group (n = 6) was measured by one-step quantitative RT-PCR during the whole period. A log10 transformed value of RNA copies per mL is shown. **C** The ratio of viral rebound during ART between the two groups. **D** The fold changes of peak plasma viral load (VL) relative to baseline (VL_{83dpi}) between the two groups. *P* values were obtained from Mann–Whitney test. **E** The variation in plasma viral load between the two groups before (62 dpi.) and after combination treatment (145 dpi.). *P* values were obtained from paired *t* test. The area shaded in orange represents ART administration, and the area shaded in cross grains represents the treatment of 25HC alone or vehicle. All average data are presented as the mean ± SEM. *, $P < 0.05$.

these data indicated that 25HC alone may not be sufficient to suppress the viremia in SIV-infected RMs, but 25HC combined with ART may be helpful in controlling viremia at a lower level after viral rebound in RMs.

25HC Combined with ART Restored the Ratio of CD4/CD8 Lymphocytes and Regulated the Differentiation of T Lymphocytes in SIV-Infected RMs

We then determined how 25HC affects the quantity and quality of T cells *in vivo* in the RM model. The ratio of CD4/CD8 is considered to be an important indicator in predicting the progression of HIV disease (Spann and Glass 2013). The high baseline CD4/CD8 ratio was associated with immune reconstitution success (Mussini *et al.* 2015). Interestingly, we found that the CD4/CD8 ratio of RMs in the 25HC + ART group was significantly increased, and higher than that of the ART-only group (Fig. 3A) (Supplementary Table S3). These results showed that 25HC combined with ART restores the CD4/CD8 ratio, which is helpful for immune reconstitution.

It is generally considered that the hyperactivation of $CD4^+$ T cells might provide more susceptible targets for HIV-1 acquisition. To investigate the activating status of $CD4^+$ T cells by 25HC, we detected the expression of CCR5, CD69, and Ki67 on the surface of CD4 cells. In this study, there was a trend towards reduced expression of CCR5 on the surface of $CD4^+$ T cells in RMs that received both 25HC combined with ART and ART-only treatment. Notably, the average frequency of CCR5/CD4 in RMs of the 25HC + ART group decreased from 7.9% to 4.8% after getting combined treatment of 25HC and ART (Fig. 3B). The expression of CD69 on the surface of $CD4^+$ T cells in RMs was significantly decreased after 25HC combined with ART (Fig. 3C), suggesting that 25HC intervention may help reverse the overactivation of $CD4^+$ T cells. Moreover, the expression of Ki67 on the $CD4^+$ T cell surface significantly decreased in RMs that received 25HC combined with ART and ART-only (Fig. 3D). These findings suggest that 25HC combined with ART may reverse the overactivation of $CD4^+$ T cells in SIV-infected RMs.

We also determined whether the 25HC intervention can affect the activation state of $CD8^+$ T cells. The expression

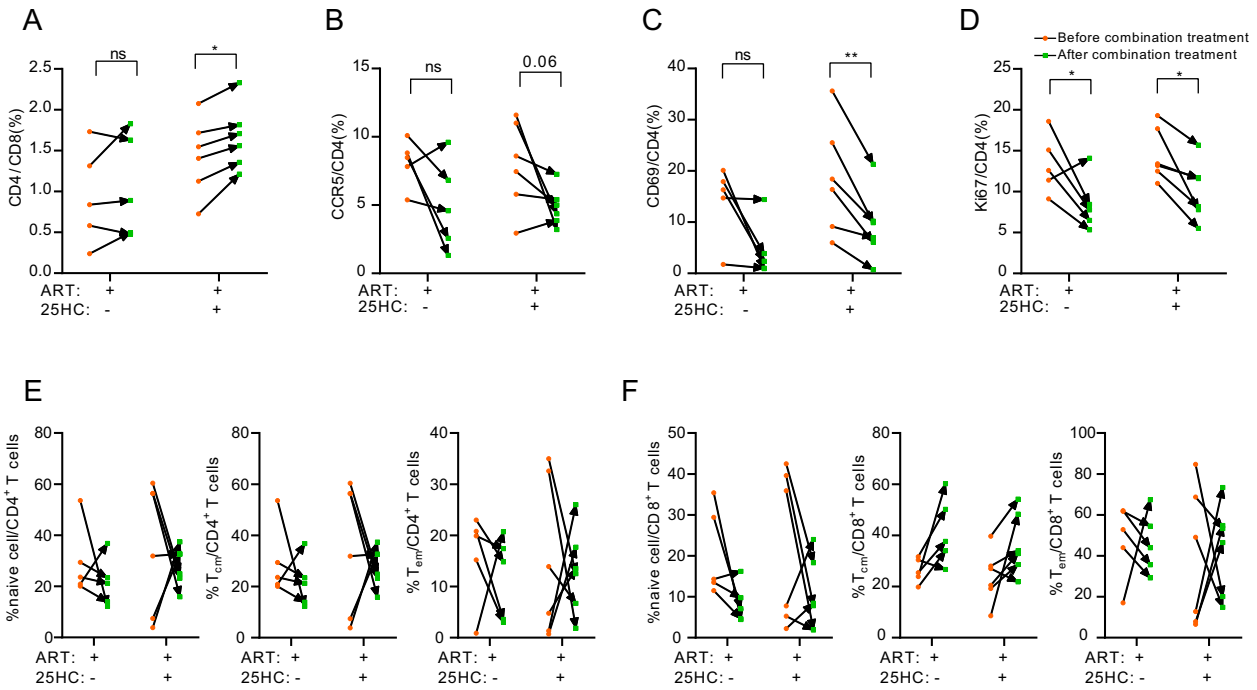

Fig. 3 25HC combined with ART restored the ratio of CD4/CD8 lymphocytes and regulated the differentiation of T lymphocytes in SIV-infected RMs. To assess the T cell number in these SIV-infected RMs, the true T cell count was measured by flow cytometry. **A** The ratio of CD4/CD8 in SIV-infected rhesus macaques before (95 dpi) and after (161 dpi) getting combination treatment. *P* values were obtained from Tukey correction for multiple comparisons analysis. **B**, **C**, **D** Expression levels of CCR5, CD69, and Ki67 in $CD4^+$ T cells before (95 dpi) and after (152 dpi) RMs were received combination treatment. *P* values were obtained from paired *t* test analysis. **E** Dynamic proportion change of naïve, T_{cm} and T_{em} $CD4^+$ T cells in PBMCs from RMs against SIV gag stimulation in this study. *P* values were obtained from unpaired *t* test. **F** Dynamic proportion change of naïve, T_{cm} and T_{em} to $CD8^+$ T cells against SIV gag stimulation along this study. *P* values were obtained from unpaired *t* test. T_{cm} represents central memory T cell, and T_{em} represents effective memory T cell. All average data are presented as the mean ± SEM. (*$P < 0.05$, **$P < 0.01$).

of CD38, PD-1, and HLA-DR on the surface of $CD8^+$ T cells was detected, and we did not find a statistically significant difference between the two groups of RMs (Supplementary Fig. S1E).

We then detected the frequency of naïve T cell subsets, central T memory subsets (T_{cm}), and effector T memory subsets (T_{em}), based on the expression levels of CD28 and CD95 as described in our previous study (Sun *et al.* 2013; Wu *et al.* 2018). In this study, there was a similar dynamic of the proportion of these three subsets in $CD4^+$ and $CD8^+$ T cells in SIV-infected RMs receiving ART with or without 25HC (Fig. 3E, 3F) (Supplementary Fig. S1A–1D).

25HC Combined with ART Improved SIV Antigen-Specific IFN-γ Production, and Selectively Attenuated Proinflammatory Cytokine Secretion in RMs

We next investigated whether 25HC therapy modulated the immune response in SIV-infected RMs, especially the antigen-specific cellular immune response. The frequency of SIV antigen-specific IFN-γ-secreting cells, determined by IFN-γ enzyme-linked immunospot assay (ELISPOT), was significantly increased in the RMs of the 25HC-combined-with-ART group compared to those of the ART-only group (Fig. 4A). Further analysis showed that these IFN-γ-mediated ELISPOT immune responses in the group of 25HC combined with ART were significantly enhanced against SIV Pol, Vpx, Vpr, Vif, Nef, Rev, and Tat peptide stimulation (Fig. 4B), while there was no significant change of immune responses against the above-mentioned peptides in the ART-only group (Fig. 4C). These data indicated that administration of 25HC during ART enhanced total IFN-γ expression and might contribute to its broad-spectrum antiviral function.

To assess how 25HC affects antigen-specific $CD4^+$ T and $CD8^+$ T cells, peripheral blood mononuclear cells (PBMCs) were isolated from RMs, and the polyfunctionality of T lymphocytes was assessed using multiparameter intracellular cytokine staining (ICS). The proportion of double and triple cytokine-secreting $CD4^+$ and $CD8^+$ T cells was increased in all the RMs after therapy (Fig. 4D, 4E). Interestingly, the frequency of TNF-α-secreting $CD4^+$ T cells and IL-2-secreting $CD8^+$ T cells was significantly decreased in RMs treated with 25HC combined ART (Fig. 4F, 4G), suggesting that 25HC may have an effect on suppressing proinflammatory cytokines, such as TNF-α and IL-2 (Upadhyay *et al.* 2020). These data demonstrated that 25HC combined with ART could enhance the total cellular responses but inhibit the proinflammatory responses by selectively suppressing the secretion of IL-2 and TNF-α in SIV-infected RMs.

Assessment of the *In Vivo* Safety and Preliminary Pharmacokinetics of 25HC in SIV-Infected RMs

While 25HC has been reported to play a critical role in the regulation of cholesterol (CHO) metabolism *in vitro*, there is a lack of related information *in vivo*. Thus, we examined how 25HC administration affected cholesterol-related lipid changes in SIV-infected RMs. After 25HC treatment, the concentration of high-density lipoprotein cholesterol (HDL-c) in RM plasma increased (Fig. 5A, 5B), and concentrations of CHO and low-density lipoprotein cholesterol (LDL-c) were significantly decreased (Fig. 5C, 5D). These results indicated that 25HC treatment did not increase the risk of atherosclerosis in SIV-infected RMs. In contrast, it may help to reverse the disorder of lipid metabolism caused by HIV/SIV infection.

We then evaluated the potential toxicity of 25HC to RMs throughout the study, including hepatic (Fig. 5E–5G), renal (Fig. 5H, 5I), and cardiotoxicity (Fig. 5J) effects. Throughout the course of the study, the change trend of the potential renal and cardiotoxicity index of RMs in the 25HC+ART group was similar to that in the ART-only group. There was no significant difference between the two groups (Fig. 5E–5K), indicating that 25HC will not cause additional toxicity to the kidney and heart. Compared to the ART-only group, the ratio of AST/ALT in RMs of 25HC+ART group was within the normal range (Yu *et al.* 2019), although there was a higher concentration of aspartate aminotransferase (AST) in the 25HC+ART group (Fig. 5F), suggesting that 25HC will not cause additional toxicity to liver. The observed higher AST concentration in the 25HC+ART group might be due to RMs' individual differences, since the concentration of AST in the 25HC+ART group was higher at the beginning of this study (42 dpi). These results demonstrated that daily infusion of 25HC (1.5 mg/kg) for one week did not cause detectable toxicity in SIV-infected RMs.

We also conducted a complete blood cell count over the course of the entire study, and the levels of white blood cells (WBCs), red blood cells (RBCs), hemoglobin (HGB), and platelets (PLTs) in RMs that received 25HC combined with ART were all within the normal reference value range after treatment (Fig. 5L–5O). However, we found that after RMs treated with 25HC combined with ART (152 dpi), the level of lymphocyte (LYM), ratio of LYM to WBC (LYM/WBC), monocyte (MONO), ratio of MONO to WBC (MONO/WBC), and basophil (BASO) were significantly lower than that of RMs who received ART alone (Supplementary Fig. S2A–S2F). The level of neutrophils (NEU), ratio of NEU to WBC (NEU/WBC), eosinophil (EOS), and ratio of EOS to WBC (EOS/WBC) were significantly higher than that of RMs who received ART alone

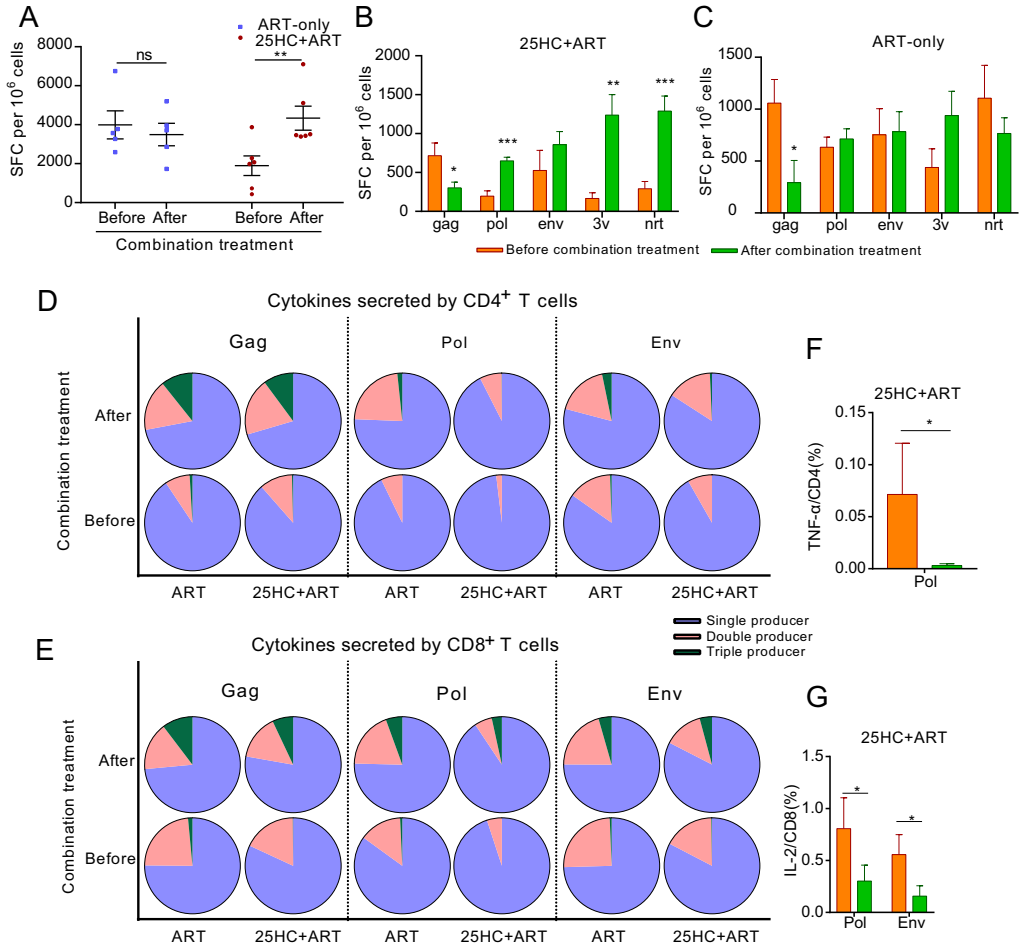

Fig. 4 25HC combined with ART improved SIV antigen-specific IFN-γ production, and selectively attenuated proinflammatory cytokine secretion in RMs. **A** The frequency of SIV antigen-specific IFN-γ-secreting cells was determined by IFN-γ ELISPOT assay before (119 dpi.) and after combination treatment (154 dpi.). *P* values were obtained from paired *t* test analysis. **B**, **C** Antigen-specific immune responses against different SIV antigen stimulations in SIV-infected rhesus macaques. *P* values were obtained from paired *t* test analysis. **D**, **E** The percentage of single-, double-, and triple-cytokine secretion by $CD4^+$ and $CD8^+$ T cells under SIV gag/pol/env stimulation before (42 dpi.) and after combination treatment (138 dpi) in two groups. **F** The percentage of TNF-α secreted by $CD4^+$ T cells under SIV pol stimulation before (42 dpi) and after combination treatment (138 dpi) in 25HC+ART group. *P* values were obtained from Tukey's multiple comparisons test. **G** The proportion of IL-2 secreted by $CD8^+$ T cells under SIV pol and env stimulation before (42 dpi.) and after combination treatment (138 dpi) in 25HC + ART group. *P* values were obtained from Tukey's multiple comparisons test. All average data are presented as the mean ± SEM. (*$P < 0.05$, ** $P < 0.01$, *** $P < 0.001$)

(Supplementary Fig. S2G–S2J). Although the lymphocyte value of the 25HC+ART group was lower than the normal standard, the rate of decrease in the lymphocyte value before (95 dpi) and after (126 dpi) combined treatment was lower than that of the ART-only group, indicating that the number of lymphocytes in the 25HC+ART group was more stable. The level of monocytes (MONO), and the ratio of MONO to WBCs (MONO/WBCs) were all in the normal range. The concentration of hematocrit (HCT), mean corpuscular volume (MCV), mean corpuscular hemoglobin (MCH), mean corpuscular hemoglobin concentration (MCHC), red cell distribution width (RDW), and mean platelet volume (MPV) in peripheral blood of all RMs were almost no different between the two groups (Supplementary Fig. S2K–S2P), but MCV and MCHC deviated from the normal value, suggesting that chronically SIV-infected RMs may have anemia (Lee *et al.* 2012). These data showed that 25HC had no significant effect on the cell composition of peripheral blood in SIV-infected macaques.

To track the preliminary pharmacokinetics of 25HC in RMs, we collected blood from 6 RMs at different time points after they received 25HC intravenous infusion and monitored the changes in 25HC concentration (Fig. 5P). We found that the concentration of 25HC in plasma peaked one hour after intravenous infusion, then gradually decreased and fell to almost the same level as the initial concentration 3 h after 25HC intervention. After 24 h of

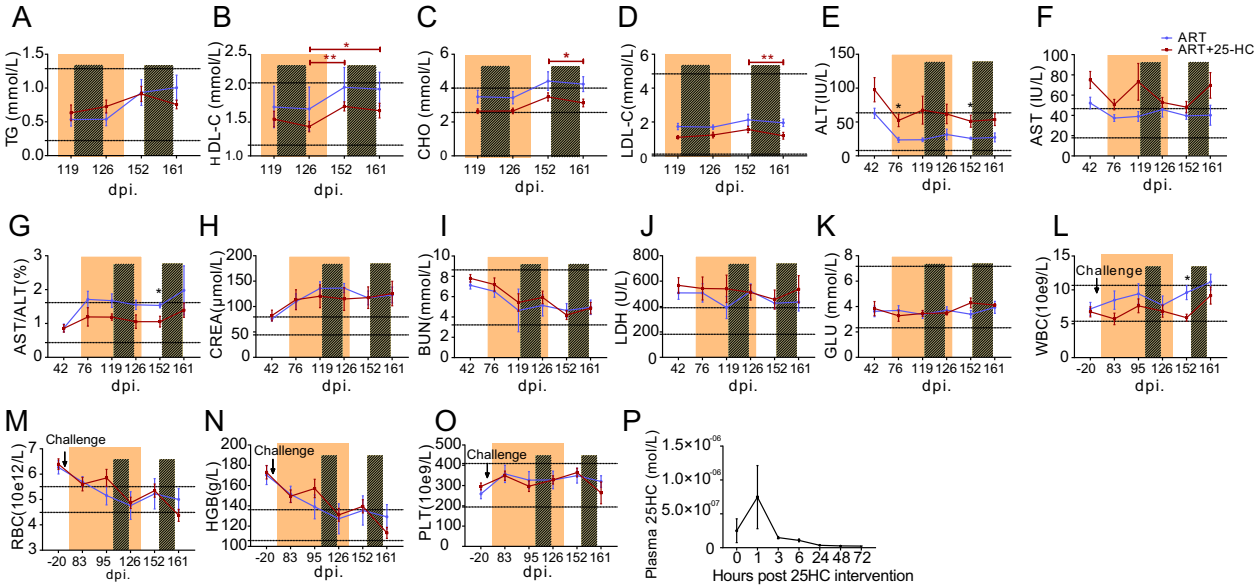

Fig. 5 The *in vivo* safety and preliminary pharmacokinetics of 25HC in SIV-infected RMs. **A, B**, **C**, **D** The dynamic changes in triglyceride (TG), high-density lipoprotein cholesterol (HDL-c), cholesterol (CHO) and low-density lipoprotein cholesterol (LDL-c) concentrations in SIV-infected RMs during this study. *P* values were obtained from unpaired *t* test. **E**, **F**, **G** The concentrations of alanine aminotransferase (ALT), aspartate aminotransferase (AST), and the ratio of ALT/AST in the plasma of RMs during this study. **H**, **I** The concentrations of creatinine (CREA) and blood urea nitrogen (BUN) in the plasma of RMs during this study. **J, K** The concentrations of lactate dehydrogenase (LDH) and glucose (GLU) in the plasma of RMs during this study. The contents of white blood cells (WBCs) (**L**), red blood cells (RBCs) (**M**), hemoglobin (HGB) (**N**), and platelets (PLTs) (**O**) in SIV-infected RMs during this study. *P* values were obtained from unpaired *t* test analysis (**E–O**). **P** The concentration of 25HC in the plasma of RMs at various time points after 25HC intervention. The *P* value was obtained from the Kruskal–Wallis test and Dunn's test. The orange-shaded area represents the ART administration, and the area shaded in the cross grain represents the treatment with 25HC alone or vehicle. All average data are presented as the mean ± SEM. (*$P < 0.05$).

drug intervention, the concentration of 25HC in plasma was at a low level, and it was maintained for at least 72 h after treatment (Fig. 5P).

Discussion

Recently, increasing data have supported the broadly antiviral activities of CH25H and 25HC (Radhakrishnan *et al.* 2004; Liu *et al.* 2013; Li *et al.* 2017; Song *et al.* 2017; Wu *et al.* 2018). However, the potential therapeutic effect of 25HC in SIV-infected RMs remains to be studied. Thus, we evaluated the effectiveness and safety of 25HC in a chronically SIV-infected RM model for the first time.

Anti-inflammatory therapy is helpful for immune reconstruction in chronically HIV-1 patients, due to persistent inflammation and abnormal immune activation during HIV-1 infection. However, the exact roles of 25HC in modulating the inflammatory responses are still under extensive investigation. Some studies reported that 25HC inhibited the production of interleukin-1 family cytokines and inflammatory body activity (Reboldi *et al.* 2014; Dang *et al.* 2017; Ouyang *et al.* 2018), but another study found that 25HC promoted the secretion of inflammatory cytokines (Gold *et al.* 2014). In this study, our *in vivo* data in SIV-infected RMs showed that the proinflammatory secretion of SIV-specific IL-2 and TNF-α was selectively inhibited after 25HC treatment. Interestingly, there was no significant effect on the secretion of SIV-specific IFN-γ by $CD4^+$ and $CD8^+$ T cells, which has a direct antiviral function (Bovolenta *et al.* 1999; Papasavvas *et al.* 2019). Given that no significant change was found in the secretion of SIV-specific IFN-γ by $CD4^+$ T cells and $CD8^+$ T cells after 25HC treatment, we hypothesized that the enhancement of SIV-specific IFN-γ by ELISPOT assay might be mainly released by other innate immune cells including natural killer (NK) cells and macrophages *etc*., and the IFN-γ secretion by these innate immune cells was thought to be associated with delayed disease progression (Jiang *et al.* 2013). Consistent with our hypothesis, it was reported that 25HC induced the IFN-γ expression by macrophages in a liver X receptor (LXR)-dependent manner, and the increased IFN-γ subsequently promoted CH25H expression (Liu *et al.* 2018) and 25HC production (Diczfalusy *et al.* 2009). In addition, $CD4^+$ T cells are the main target of HIV/SIV infection (Clapham *et al.* 1993); therefore, chronic HIV-1 infection and disease progression are usually accompanied by a decrease in the number of $CD4^+$ T

cells and the ratio of CD4/CD8 (Maina *et al.* 2015; Bruno *et al.* 2017; Mutoh *et al.* 2018). Of note, we found that the ratio of CD4/CD8 was significantly increased in SIV-infected RMs after receiving 25HC combined with ART. Overall, these immunological benefits are represented as a good predictor to control the progression of AIDS.

Reminiscent of the ongoing coronavirus disease 2019 (COVID-19) pandemic worldwide, lymphopenia and inflammatory cytokine storms are often observed in highly pathogenic coronavirus infections(such as severe acute respiratory syndrome (SARS), Middle East respiratory syndrome coronavirus (MERS), and COVID-19), and are related to the severity of the disease (Chen *et al.* 2020; Wang *et al.* 2020). However, how different lymphocyte subpopulations and inflammatory cytokine dynamics change in peripheral blood during SARS-CoV-2 infection remains largely unclear (Cuadrado *et al.* 2020; Liu *et al.* 2020). The anti-inflammatory role of 25HC may have effects on the inhibition of inflammatory cytokines storm in COVID-19 patients. In fact, our recent study showed that 25HC was upregulated in severe COVID-19 patients, and 25HC treatment inhibited SARS-CoV-2 infection *in vitro* and in humanized ACE2 mice (Zu *et al.* 2020). As a result, further exploration of the therapeutic effect of 25HC in COVID-19 patients is warranted.

In part due to its ability to inhibit cholesterol biosynthesis (Brown *et al.* 1975; Brown and Goldstein 1997; Adams *et al.* 2004), 25HC is considered an important antiviral molecule (Schoggins and Randall 2013; Lv *et al.* 2019). Manipulating cellular cholesterol levels is an important process in host and virus interactions. HIV-1 patients receiving long-term antiretroviral therapy are usually observed to have dyslipidemia (Maggi *et al.* 2017), and a recent study reported that the lipid mass spectrum was significantly changed in HIV-1 patients (Koethe *et al.* 2020). Compared with healthy people, HIV-1 patients have higher levels of triglycerides and total cholesterol, while high-density lipoprotein (HDL) cholesterol levels are lower (Bernal *et al.* 2008), leading to an increased incidence of cardiovascular disease. Epidemiological data have confirmed an independent positive association between LDL-c and cardiovascular disease risk (Chen *et al.* 1991; Stamler *et al.* 1993), and the level of cholesterol is strongly associated with the risk of atherosclerosis and cardiovascular disease (McGill *et al.* 2008; Gidding *et al.* 2016; Ference *et al.* 2017). Our study showed that the concentration of plasma HDL-c was increased, and the concentrations of cholesterol and LDL-c were significantly decreased when RMs were receiving 25HC treatment. These results indicated that 25HC intervention may have an effect on inhibiting cholesterol biosynthesis, and thus might reduce the risk of cardiovascular disease in HIV-1 chronically infected patients. In addition, 25HC was metabolized within three hours in RMs, and its concentration decreased to a much lower level than that before treatment at 24 h, and this continued at least until 72 h after administration. Due to the complexity of cholesterol metabolism (Hewing and Landmesser 2015), the reasons for this observation need to be further examined. Our findings provide a new way to control HIV-1 infection by regulating cholesterol metabolism.

This study has some limitations. First, RMs recruited in this study had a wide range of ages. To minimize the possible effect of age, we divided these animals into two groups based on average age and the initial immune status to SIV antigens. Second, only 11 RMs were enrolled in this study, and the animal number may be enlarged in future studies to confirm our results. In this study, we found that 25HC combined with ART was helpful in controlling viremia at a lower level after viral rebound in SIV-infected RMs. Our data also showed that 25HC alone may not be sufficient to suppress viremia in SIV-infected RMs. The exact mechanism for this observation is still unknown. One possible explanation might be the low dosage of 25HC employed in this study. Because of the relatively small number of experimental animals, we did not study the dose-dependent effectiveness of 25HC in this study, but under the current conditions, 25HC treatment was effective when combined with ART, possibly because of a synergistic interaction. Importantly, our data also showed that

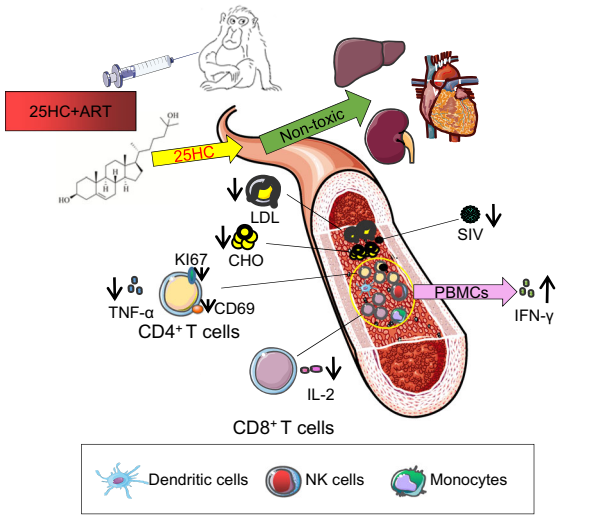

Fig. 6 Pattern to illustrate the role of 25HC in controlling SIV infection. In this study, 25HC showed no toxicity to the liver, heart or kidney in SIV-infected RMs. The 25HC + ART regiment promoted the secretion of SIV-specific IFN-γ but suppressed the secretion of inflammatory cytokines, reversed the hyperactive state of $CD4^+$ T cells, and restored CD4/CD8 T cell ratio in SIV-infected RMs. Furthermore, 25HC combined with ART reduced the concentration of total cholesterol and low-density lipoprotein in plasma. Overall, these immunological and metabolic benefits are helpful in controlling viral replication and suppressing the progression of AIDS.

the 25HC compound has potential druggability with *in vivo* safety and preliminary pharmacokinetics studies. Nevertheless, given the multifaceted functions of 25HC in inhibiting viral infection, promoting lipid metabolism, and modulating immunity, we should further examine the potential of this drug in preclinical and clinical studies.

In summary, our results suggested that the regimen of 25HC combined with ART provided a profound modulation of virological and immunological benefits in chronically SIV-infected, ART-treated RMs, including suppressing viral rebound, enhancing SIV-specific cellular immune responses, restoring the CD4/CD8 T cell ratio, and inhibiting proinflammatory cytokine secretion in a nonhuman primate model (Fig. 6). This study helps explain the antiviral activity of 25HC and provides new insights into the development of novel immunotherapeutic strategies against HIV-1 infection and other related diseases.

Acknowledgements We thank Yichu Liu and Xiangjie Feng for technical assistance in the RMs experiment. We appreciate the NIH AIDS Research and Reference Reagent Program for providing SIV peptide pools. This work was supported by the National Natural Science Foundation of China (81971927, 31870912, 32000124), the National Science and Technology Major Project of China (2018ZX10731101-002), the National Key Research and Development Program of China (2018YFA0900803), the Science and Technology Planning Project of Shenzhen City (20190804095916056, JCYJ20200109142601702), the High Level Project of Medicine in Longhua, Shenzhen (HLPM201907020105), China Postdoctoral Science Foundation (Grant No. 2019M663140), and the Municipal Health and Medical cooperation innovation Major Project of Guangzhou City (201704020219, 201803040002).

Author Contributions CS and PL designed and supervised the project; CW, JZ, RL, and CS collected literature and drafted the original manuscript; CW, JZ, RL, PL, RH, and YH performed the experiment; CW, JZ, and RL analyzed the data; HY, GC, FM, and LC contributed the materials and reagents. All authors have read and agreed to the final version of the manuscript.

Compliance with Ethical Standards

Animal and Human Rights Statement This study was carried out in accordance with the "Regulations for the Administration of Affairs Concerning Experimental Animals" by the State Council of the People's Republic of China, and the protocol was approved by the Institutional Animal Care and Use Committee of GIBH (IACUC Permit Number: 2019052).

Conflict of interest The authors declare that they have no conflicts of interest. The funders had no role in study design, data collection and analysis, decision to publish, or preparation of the manuscript.

References

Aberg JA, Gallant JE, Ghanem KG, Emmanuel P, Zingman BS, Horberg MA (2014) Primary care guidelines for the management of persons infected with HIV: 2013 update by the HIV medicine association of the Infectious Diseases Society of America. Clin Infect Dis 58:e1-34

Adams CM, Reitz J, De Brabander JK, Feramisco JD, Li L, Brown MS, Goldstein JL (2004) Cholesterol and 25-hydroxycholesterol inhibit activation of SREBPs by different mechanisms, both involving SCAP and Insigs. J Biol Chem 279:52772–52780

Bernal E, Masiá M, Padilla S, Gutiérrez F (2008) High-density lipoprotein cholesterol in HIV-infected patients: evidence for an association with HIV-1 viral load, antiretroviral therapy status, and regimen composition. AIDS Patient Care STDS 22:569–575

Bovolenta C, Lorini AL, Mantelli B, Camorali L, Novelli F, Biswas P, Poli G (1999) A selective defect of IFN-gamma- but not of IFN-alpha-induced JAK/STAT pathway in a subset of U937 clones prevents the antiretroviral effect of IFN-gamma against HIV-1. J Immunol 162:323–330

Brown MS, Dana SE, Goldstein JL (1975) Cholesterol ester formation in cultured human fibroblasts. Stimulation by oxygenated sterols. J Biol Chem 250:4025–4027

Brown MS, Goldstein JL (1997) The SREBP pathway: regulation of cholesterol metabolism by proteolysis of a membrane-bound transcription factor. Cell 89:331–340

Bruno G, Saracino A, Monno L, Angarano G (2017) The revival of an "Old" marker: CD4/CD8 ratio. AIDS Rev 19:81–88

Chen N, Zhou M, Dong X, Qu J, Gong F, Han Y, Qiu Y, Wang J, Liu Y, Wei Y, Xia J, Yu T, Zhang X, Zhang L (2020) Epidemiological and clinical characteristics of 99 cases of 2019 novel coronavirus pneumonia in Wuhan, China: a descriptive study. Lancet 395:507–513

Chen Z, Peto R, Collins R, MacMahon S, Lu J, Li W (1991) Serum cholesterol concentration and coronary heart disease in population with low cholesterol concentrations. BMJ 303:276–282

Churchill MJ, Deeks SG, Margolis DM, Siliciano RF, Swanstrom R (2016) HIV reservoirs: what, where and how to target them. Nat Rev Microbiol 14:55–60

Clapham P, McKnight A, Simmons G, Weiss R (1993) Is CD4 sufficient for HIV entry? Cell surface molecules involved in HIV infection. Philos Trans R Soc Lond B Biol Sci 342:67–73

Cuadrado A, Pajares M, Benito C, Jiménez-Villegas J, Escoll M, Fernández-Ginés R, Garcia Yagüe AJ, Lastra D, Manda G, Rojo AI, Dinkova-Kostova AT (2020) Can Activation of NRF2 Be a Strategy against COVID-19? Trends Pharmacol Sci. https://doi.org/10.1016/j.tips.2020.07.003

Dang EV, McDonald JG, Russell DW, Cyster JG (2017) Oxysterol restraint of cholesterol synthesis prevents AIM2 inflammasome activation. Cell 171:1057-1071.e1011

Diczfalusy U, Olofsson KE, Carlsson AM, Gong M, Golenbock DT, Rooyackers O, Fläring U, Björkbacka H (2009) Marked upregulation of cholesterol 25-hydroxylase expression by lipopolysaccharide. J Lipid Res 50:2258–2264

Doms A, Sanabria T, Hansen JN, Altan-Bonnet N, Holm GH (2018) 25-hydroxycholesterol production by the cholesterol-25-hydroxylase interferon-stimulated gene restricts mammalian reovirus infection. J Virol 92:e01047–18

Ference BA, Ginsberg HN, Graham I, Ray KK, Packard CJ, Bruckert E, Hegele RA, Krauss RM, Raal FJ, Schunkert H, Watts GF, Borén J, Fazio S, Horton JD, Masana L, Nicholls SJ, Nordestgaard BG, van de Sluis B, Taskinen MR, Tokgözoglu L, Landmesser U, Laufs U, Wiklund O, Stock JK, Chapman MJ, Catapano AL (2017) Low-density lipoproteins cause atherosclerotic cardiovascular disease. 1. Evidence from genetic, epidemiologic, and clinical studies. A consensus statement from the European Atherosclerosis Society Consensus Panel. Eur Heart J 38:2459–2472

Freiberg MS, Chang CC, Kuller LH, Skanderson M, Lowy E, Kraemer KL, Butt AA, Bidwell Goetz M, Leaf D, Oursler KA,

Rimland D, Rodriguez Barradas M, Brown S, Gibert C, McGinnis K, Crothers K, Sico J, Crane H, Warner A, Gottlieb S, Gottdiener J, Tracy RP, Budoff M, Watson C, Armah KA, Doebler D, Bryant K, Justice AC (2013) HIV infection and the risk of acute myocardial infarction. JAMA Intern Med 173:614–622

Gidding SS, Rana JS, Prendergast C, McGill H, Carr JJ, Liu K, Colangelo LA, Loria CM, Lima J, Terry JG, Reis JP, McMahan CA (2016) Pathobiological determinants of atherosclerosis in youth (PDAY) risk score in young adults predicts coronary artery and abdominal aorta calcium in middle age: The CARDIA study. Circulation 133:139–146

Glass CK, Saijo K (2010) Nuclear receptor transrepression pathways that regulate inflammation in macrophages and T cells. Nat Rev Immunol 10:365–376

Gold ES, Diercks AH, Podolsky I, Podyminogin RL, Askovich PS, Treuting PM, Aderem A (2014) 25-Hydroxycholesterol acts as an amplifier of inflammatory signaling. Proc Natl Acad Sci U S A 111:10666–10671

Grand M, Bia D, Diaz A (2020) Cardiovascular risk assessment in people living With HIV: a systematic review and meta-analysis of real-life data. Curr HIV Res 18:5–18

Hewing B, Landmesser U (2015) LDL, HDL, VLDL, and CVD prevention: lessons from genetics? Curr Cardiol Rep 17:610

Jiang Y, Zhou F, Tian Y, Zhang Z, Kuang R, Liu J, Han X, Hu Q, Xu J, Shang H (2013) Higher NK cell IFN-γ production is associated with delayed HIV disease progression in LTNPs. J Clin Immunol 33:1376–1385

Kimata JT, Rice AP, Wang J (2016) Challenges and strategies for the eradication of the HIV reservoir. Curr Opin Immunol 42:65–70

Koethe JR, Lagathu C, Lake JE, Domingo P, Calmy A, Falutz J, Brown TT, Capeau J (2020) HIV and antiretroviral therapy-related fat alterations. Nat Rev Dis Primers 6:48

Lee JI, Shin JS, Lee JE, Jung WY, Lee G, Kim MS, Park CG, Kim SJ (2012) Reference values of hematology, chemistry, electrolytes, blood gas, coagulation time, and urinalysis in the Chinese rhesus macaques (Macaca mulatta). Xenotransplantation 19:244–248

Lehmann JM, Kliewer SA, Moore LB, Smith-Oliver TA, Oliver BB, Su JL, Sundseth SS, Winegar DA, Blanchard DE, Spencer TA, Willson TM (1997) Activation of the nuclear receptor LXR by oxysterols defines a new hormone response pathway. J Biol Chem 272:3137–3140

Li C, Deng YQ, Wang S, Ma F, Aliyari R, Huang XY, Zhang NN, Watanabe M, Dong HL, Liu P, Li XF, Ye Q, Tian M, Hong S, Fan J, Zhao H, Li L, Vishlaghi N, Buth JE, Au C, Liu Y, Lu N, Du P, Qin FX, Zhang B, Gong D, Dai X, Sun R, Novitch BG, Xu Z, Qin CF, Cheng G (2017) 25-hydroxycholesterol protects host against zika virus infection and its associated microcephaly in a mouse model. Immunity 46:446–456

Liu J, Li S, Liu J, Liang B, Wang X, Wang H, Li W, Tong Q, Yi J, Zhao L, Xiong L, Guo C, Tian J, Luo J, Yao J, Pang R, Shen H, Peng C, Liu T, Zhang Q, Wu J, Xu L, Lu S, Wang B, Weng Z, Han C, Zhu H, Zhou R, Zhou H, Chen X, Ye P, Zhu B, Wang L, Zhou W, He S, He Y, Jie S, Wei P, Zhang J, Lu Y, Wang W, Zhang L, Li L, Zhou F, Wang J, Dittmer U, Lu M, Hu Y, Yang D, Zheng X (2020) Longitudinal characteristics of lymphocyte responses and cytokine profiles in the peripheral blood of SARS-CoV-2 infected patients. EBioMedicine 55:102763

Liu SY, Aliyari R, Chikere K, Li G, Marsden MD, Smith JK, Pernet O, Guo H, Nusbaum R, Zack JA, Freiberg AN, Su L, Lee B, Cheng G (2013) Interferon-inducible cholesterol-25-hydroxylase broadly inhibits viral entry by production of 25-hydroxycholesterol. Immunity 38:92–105

Liu Y, Wei Z, Zhang Y, Ma X, Chen Y, Yu M, Ma C, Li X, Cao Y, Liu J, Han J, Yang X, Duan Y (2018) Activation of liver X receptor plays a central role in antiviral actions of 25-hydroxycholesterol. J Lipid Res 59:2287–2296

Ludigs K, Parfenov V, Du Pasquier RA, Guarda G (2012) Type I IFN-mediated regulation of IL-1 production in inflammatory disorders. Cell Mol Life Sci 69:3395–3418

Lund EG, Kerr TA, Sakai J, Li WP, Russell DW (1998) cDNA cloning of mouse and human cholesterol 25-hydroxylases, polytopic membrane proteins that synthesize a potent oxysterol regulator of lipid metabolism. J Biol Chem 273:34316–34327

Lv L, Zhao G, Wang H, He H (2019) Cholesterol 25-Hydroxylase inhibits bovine parainfluenza virus type 3 replication through enzyme activity-dependent and -independent ways. Vet Microbiol 239:108456

Maggi P, Di Biagio A, Rusconi S, Cicalini S, D'Abbraccio M, d'Ettorre G, Martinelli C, Nunnari G, Sighinolfi L, Spagnuolo V, Squillace N (2017) Cardiovascular risk and dyslipidemia among persons living with HIV: a review. BMC Infect Dis 17:551

Maina EK, Bonney EY, Bukusi EA, Sedegah M, Lartey M, Ampofo WK (2015) CD4+ T cell counts in initiation of antiretroviral therapy in HIV infected asymptomatic individuals; controversies and inconsistencies. Immunol Lett 168:279–284

McGill HC Jr, McMahan CA, Gidding SS (2008) Preventing heart disease in the 21st century: implications of the Pathobiological Determinants of Atherosclerosis in Youth (PDAY) study. Circulation 117:1216–1227

Mussini C, Lorenzini P, Cozzi-Lepri A, Lapadula G, Marchetti G, Nicastri E, Cingolani A, Lichtner M, Antinori A, Gori A, d'Arminio Monforte A (2015) CD4/CD8 ratio normalisation and non-AIDS-related events in individuals with HIV who achieve viral load suppression with antiretroviral therapy: an observational cohort study. Lancet HIV 2:e98-106

Mutoh Y, Nishijima T, Inaba Y, Tanaka N, Kikuchi Y, Gatanaga H, Oka S (2018) Incomplete recovery of CD4 cell count, CD4 percentage, and CD4/CD8 ratio in patients with human immunodeficiency virus infection and suppressed viremia during long-term antiretroviral therapy. Clin Infect Dis 67:927–933

Ouyang W, Zhou H, Liu C, Wang S, Han Y, Xia J, Xu F (2018) 25-Hydroxycholesterol protects against acute lung injury via targeting MD-2. J Cell Mol Med 22:5494–5503

Pan E, Feng F, Li P, Yang Q, Ma X, Wu C, Zhao J, Yan H, Chen R, Chen L, Sun C (2018) Immune protection of SIV challenge by PD-1 blockade during vaccination in rhesus monkeys. Front Immunol 9:2415

Papasavvas E, Azzoni L, Kossenkov AV, Dawany N, Morales KH, Fair M, Ross BN, Lynn K, Mackiewicz A, Mounzer K, Tebas P, Jacobson JM, Kostman JR, Showe L, Montaner LJ (2019) NK response correlates with HIV decrease in pegylated IFN-α2a-treated antiretroviral therapy-suppressed subjects. J Immunol 203:705–717

Premeaux TA, Javandel S, Hosaka KRJ, Greene M, Therrien N, Allen IE, Corley MJ, Valcour VG, Ndhlovu LC (2020) Associations between plasma immunomodulatory and inflammatory mediators with VACS index scores among older hiv-infected adults on antiretroviral therapy. Front Immunol 11:1321

Radhakrishnan A, Sun LP, Kwon HJ, Brown MS, Goldstein JL (2004) Direct binding of cholesterol to the purified membrane region of SCAP: mechanism for a sterol-sensing domain. Mol Cell 15:259–268

Reboldi A, Dang EV, McDonald JG, Liang G, Russell DW, Cyster JG (2014) Inflammation. 25-Hydroxycholesterol suppresses interleukin-1-driven inflammation downstream of type I interferon. Science 345:679–684

Schoggins JW, Randall G (2013) Lipids in innate antiviral defense. Cell Host Microbe 14:379–385

Shrivastava-Ranjan P, Bergeron É, Chakrabarti AK, Albariño CG, Flint M, Nichol ST, Spiropoulou CF (2016)

25-hydroxycholesterol inhibition of lassa virus infection through aberrant GP1 Glycosylation. mBio 7:e01808–16

Song Z, Zhang Q, Liu X, Bai J, Zhao Y, Wang X, Jiang P (2017) Cholesterol 25-hydroxylase is an interferon-inducible factor that protects against porcine reproductive and respiratory syndrome virus infection. Vet Microbiol 210:153–161

Spann NJ, Glass CK (2013) Sterols and oxysterols in immune cell function. Nat Immunol 14:893–900

Stamler J, Vaccaro O, Neaton JD, Wentworth D (1993) Diabetes, other risk factors, and 12-yr cardiovascular mortality for men screened in the Multiple Risk Factor Intervention Trial. Diabetes Care 16:434–444

Sun C, Chen Z, Tang X, Zhang Y, Feng L, Du Y, Xiao L, Liu L, Zhu W, Chen L, Zhang L (2013) Mucosal priming with a replicating-vaccinia virus-based vaccine elicits protective immunity to simian immunodeficiency virus challenge in rhesus monkeys. J Virol 87:5669–5677

Sun C, Zhang L, Zhang M, Liu Y, Zhong M, Ma X, Chen L (2010) Induction of balance and breadth in the immune response is beneficial for the control of SIVmac239 replication in rhesus monkeys. J Infect 60:371–381

UNAIDS Global HIV Statistics Data (2020). https://www.unaids.org/en/topic/data

Upadhyay J, Tiwari N, Ansari MN (2020) Role of inflammatory markers in corona virus disease (COVID-19) patients: a review. Exp Biol Med (maywood) 245:1368–1375

Wang D, Hu B, Hu C, Zhu F, Liu X, Zhang J, Wang B, Xiang H, Cheng Z, Xiong Y, Zhao Y, Li Y, Wang X, Peng Z (2020) Clinical characteristics of 138 hospitalized patients with 2019 novel coronavirus-infected pneumonia in Wuhan, China. JAMA 323:1061–1069

Wong JK, Hezareh M, Günthard HF, Havlir DV, Ignacio CC, Spina CA, Richman DD (1997) Recovery of replication-competent HIV despite prolonged suppression of plasma viremia. Science 278:1291–1295

Wu T, Ma F, Ma X, Jia W, Pan E, Cheng G, Chen L, Sun C (2018) Regulating Innate and Adaptive Immunity for Controlling SIV Infection by 25-Hydroxycholesterol. Front Immunol 9:2686

Yu W, Hao X, Yang F, Ma J, Zhao Y, Li Y, Wang J, Xu H, Chen L, Liu Q, Duan S, Yang Y, Huang F, He Z (2019) Hematological and biochemical parameters for Chinese rhesus macaque. PLoS ONE 14:e0222338

Yuan Y, Wang Z, Tian B, Zhou M, Fu ZF, Zhao L (2019) Cholesterol 25-hydroxylase suppresses rabies virus infection by inhibiting viral entry. Arch Virol 164:2963–2974

Zhao J, Chen J, Li M, Chen M, Sun C (2020) Multifaceted functions of CH25H and 25HC to modulate the lipid metabolism, immune responses, and broadly antiviral activities. Viruses 12:727

Zu S, Deng YQ, Zhou C, Li J, Li L, Chen Q, Li XF, Zhao H, Gold S, He J, Li X, Zhang C, Yang H, Cheng G, Qin CF (2020) 25-Hydroxycholesterol is a potent SARS-CoV-2 inhibitor. Cell Res 30:1043–1045